



Pancreas fat quantification with quantitative CT: an MRI correlation analysis

W.J. Yao^{a,b}, Z. Guo^c, L. Wang^c, K. Li^c, L. Saba^d, G. Guglielmi^e, X.G. Cheng^c, J.K. Brown^f, G.M. Blake^g, B. Liu^{a,*}

^a Department of Radiology, The First Affiliated Hospital of Anhui Medical University, Hefei, Anhui, China

^b Department of Radiology, The Second Affiliated Hospital of Anhui Medical University, Hefei, Anhui, China

^c Department of Radiology, Beijing Jishuitan Hospital, Beijing, 100035, China

^d Department of Radiology, Policlinico Universitario, Cagliari, Italy

^e Department of Clinical and Experimental Medicine, Foggia University School of Medicine, Foggia, Italy

^f Mindways Software Inc., Austin, TX, USA

^g Biomedical Engineering Department, King's College London, Strand, London, WC2R 2LS, UK

ARTICLE INFORMATION

Article history:

Received 3 May 2019

Accepted 23 December 2019

AIM: To assess the fat content of the pancreas using quantitative computed tomography (QCT) and to correlate the results with chemical-shift-encoded magnetic resonance imaging (CSE-MRI) measurements of proton density fat fraction (PDFF).

MATERIAL AND METHODS: Institutional review board approval for this research was obtained and 52 participants (25 men, 27 women; mean age 35.1 years; age range 22–50 years), who were enrolled in the Prospective Urban Rural Epidemiology (PURE) Study, underwent QCT and CSE-MRI for quantification of fat content in the pancreas. Two observers placed regions of interest (area of 100–130 mm²) in the head, body, and tail of the pancreas as closely matched as possible on the two scans. Pearson correlation and Bland–Altman analysis were performed to evaluate the correlation between the QCT and CSE-MRI measurements and the systematic difference between the two techniques.

RESULTS: The QCT and CSE-MRI measurements of pancreatic fat content were well correlated ($r=0.805$, $p<0.0001$), although Bland–Altman analysis showed that the QCT measurements were systematically lower by 6.3% compared to CSE-MRI PDFF.

CONCLUSION: In conclusion, the results of this study suggest good correlation between QCT and CSE-MRI measurements of pancreatic fat content. Further studies are required to improve the numerical agreement of QCT measurements with PDFF.

© 2020 The Royal College of Radiologists. Published by Elsevier Ltd. All rights reserved.

* Guarantor and correspondent: B. Liu, Department of Radiology, The First Affiliated Hospital of Anhui Medical University, 218 Jixi Road, Hefei, 230000, Anhui, China. Tel.: +86 13955167161.

E-mail address: Lbhyz321@126.com (B. Liu).

Introduction

Fat deposition in the pancreas (also known as non-alcoholic fatty pancreatic disease [NAFPD]) is a condition with increasing worldwide incidence linked to the increase in obesity.^{1–3} When NAFPD occurs the accumulation of fat cells replaces the pancreatic parenchyma leading to the occurrence of metabolic syndrome and type 2 diabetes mellitus due to decreased insulin secretion from the reduced number of pancreatic cells.^{4,5}

The identification of this condition is important for the development of early therapeutic strategies. Until recently, histopathology was considered the reference standard for quantifying pancreatic fat content, but has obvious limitations related to the complexity of biopsy of the pancreas due to its deep retroperitoneal location and the risk of sampling errors.⁶

Given the limitations of pancreatic biopsy, imaging can play a significant role in the diagnosis of NAFPD. Magnetic resonance imaging (MRI) has been advocated as the optimal technique to assess pancreatic fat content with the use of different approaches such as MR spectroscopy or chemical-shift-encoded MRI.^{7,8} New approaches in computed tomography (CT) have been introduced in recent years, in particular the use of quantitative CT (QCT). Although this technique is most commonly applied to the measurement of bone mineral density (BMD), with the same physical approach it is also possible to quantify the percentage fat content of soft tissue.⁹

The aim of this study was to measure the fat content of the pancreas using QCT and to correlate these results with CSE-MRI Dixon measurements of the pancreatic proton density fat fraction (PDFF).

Material and methods

Study design and patient population

The study was approved by the institutional review board and all the participants enrolled in the cohort were healthy volunteers recruited from the community as part of the Prospective Urban Rural Epidemiology (PURE) Study, an international study of 140,000 participants from 25 countries, of whom >40,000 were recruited in China.¹⁰ Beijing Jishuitan hospital is one of the collaborating centre of PURE in XX, and 52 participants (25 men and 27 women; age range 22–50 years; mean age of 35.1 years) from the centre participated this study. All participants underwent QCT and CSE-MRI Dixon measurements of the upper abdomen at the same day during their scheduled visit for PURE protocol after giving informed written consent to the protocol. All patients underwent a standard history and physical examination, biochemical testing, and oral glucose tolerance test. None of the participants was diagnosed with liver or pancreatic disease or dysfunction.

QCT technique

QCT examinations were performed on a Toshiba CT system (Aquilion PRIME ESX-302A, Toshiba Medical Systems Corporation, Otawara, Japan) with a QCT phantom (Mindways, Austin, TX, USA). The tube current was 250 mA, tube voltage 120 kVp and section thickness was 1 mm. QCT quantification of pancreas tissue was performed using QCT Pro 3D spine module software version 4.2. Two experienced radiologists independently placed three circular regions of interest (ROIs) manually in the pancreatic head, body, and tail in different QCT sections avoiding intra-pancreatic vessels and pancreatic ducts (Fig 1). Each ROI covered an area of approximately 100–130 mm². The head of the pancreas was defined as the area of the pancreas to the right of the superior mesenteric vein, the body of pancreas was defined as the right half of the remaining pancreatic tissue, and the tail was defined as the left half of the remaining pancreatic tissue.

QCT measurements of pancreatic tissue using the Mindways spine module software were converted into percentage fat measurements using a previously published method for measuring liver fat¹¹ and calculated using the following equation:

$$\% \text{ fat} = \left(\frac{HU_{\text{lean}} - HU_{\text{pancreas}}}{HU_{\text{lean}} - HU_{\text{fat}}} \right) * 100\% \quad (1)$$

where HU_{pancreas} is the radiodensity measurement in the pancreatic ROI and HU_{fat} and HU_{lean} the radiodensity values for 100% fat and fat-free pancreatic tissue respectively. The values of HU_{pancreas} were found by converting the BMD measurements from the Mindways scan analysis software to radiodensity values using the QCT Pro scan calibration data.¹¹ Values of HU_{fat} and HU_{lean} were found by representing fat and fat-free tissue in terms of their basis set equivalent densities of water (H₂O) and dipotassium hydrogen phosphate (K₂HPO₄; Table 1) and adjusting for tube voltage and person-to-person differences in beam hardening using scan calibration data from the QCT Pro software.¹¹ As previously described,¹¹ the fat standard was based on the chemical composition of animal fat published by Noller.¹² The lean standard was based on the atomic composition of pancreatic tissue published in ICRU Publication 46.¹³ Using these data, one of the authors (J.K.B.) used CT scanner spectral data and Mindways proprietary software to derive the equivalent densities listed in Table 1.

MRI technique

CSE-MRI examinations were performed using a 3-T MRI system (Ingenia, Philips Healthcare, Best, Netherlands). All participants underwent identical imaging protocols on the same MRI machine performed by an experienced operator. A three-point Dixon sequence was employed to quantify pancreatic fat content with the following parameters: 9.1 ms repetition time (TR), 1.33 ms echo time (TE), six

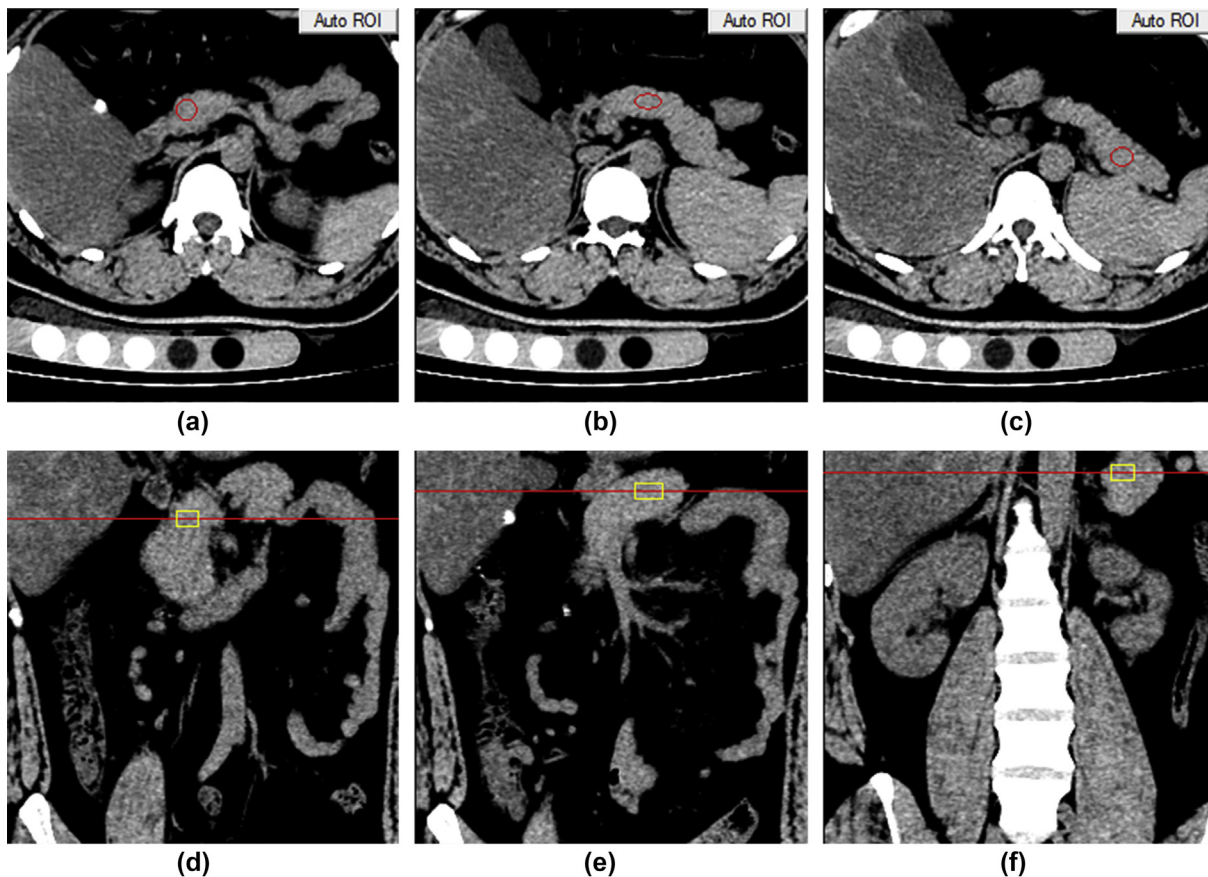


Figure 1 QCT measurement of pancreatic fat content. In the cross-sectional images, three ROIs were placed manually in the pancreatic head (a), body (b), and tail (c) avoiding intra-pancreatic vessels and pancreatic ducts. (d–f) Coronal imaging showed each ROI was surrounded by pancreatic tissue.

echos, 1.3 ms echo interval time, 180×140 mm field of view, 3° flip angle, 12.5 second scanning time. When the scan was completed, all data were transmitted to an ISP V7 workstation (Philips Healthcare, Best, Netherlands) and the same radiologists independently measured ROIs matched as closely as possible in size and location to those used in the QCT analysis (Fig 2). For both MRI and QCT measurements, the overall pancreatic fat fraction was defined as the mean of the measurements in the head, body, and tail.

For intra-observer precision, the MRI and QCT measurements were performed twice by the same author blinded to clinical information with a 2-week interval. For interobserver precision, they were performed by two authors independently. The reliability of QCT measurement in the liver has previously been validated.¹¹

To ensure good accuracy and reproducibility in the measurements, in both the QCT and MRI analysis the ROIs were placed in areas where the fat level appeared

Table 1

Basis set decomposition of fat and lean (fat-free) pancreas tissue into equivalent densities of H_2O and K_2HPO_4 .

Tissue	H_2O equivalent density (mg/cm^3)	K_2HPO_4 equivalent density (mg/cm^3)
Fat	941.75	-43.72
Lean pancreas	1038.72	-2.57

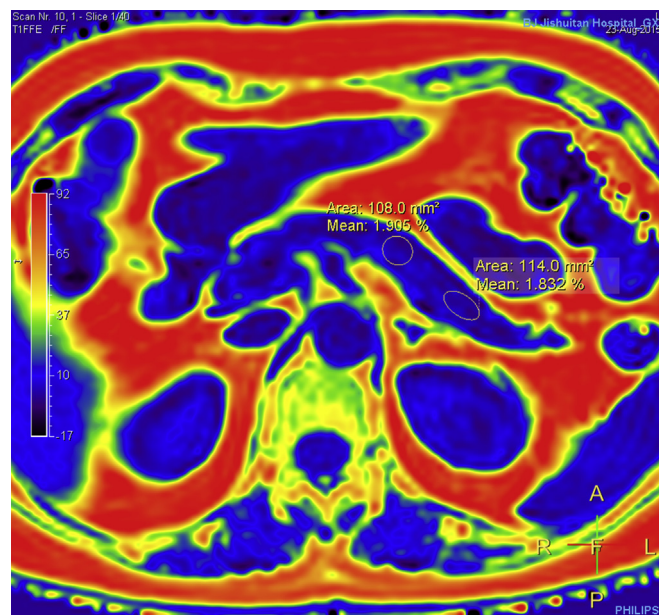


Figure 2 MRI measurement of pancreatic fat content. ROIs covering an area of approximately 100 – 130 mm^2 were placed in areas where the fat level was homogeneous, avoiding intrapancreatic vessels and pancreatic ducts.

homogeneous, avoiding intra-pancreatic vessels and pancreatic ducts. Considering that there may be more visceral fat infiltrating in the boundary of pancreas and any inter-lobular intrusion might be interpreted as intra-pancreatic fat, which could overestimate the results of the study, small ROIs were chosen (approximately 100–130 mm²) to minimise contamination from volume averaging with extra-pancreatic adipose tissue, and making sure that the ROIs were surrounded by pancreatic tissue not only within the imaging plane, but also on the section above and section below.

Statistical analysis

The normality of each continuous variable group was tested using the Kolmogorov–Smirnov *Z* test. Normally distributed data were described by the mean value and standard deviation (SD), and non-Gaussian data by the median and interquartile range. Pearson correlation analysis was performed to compare the pancreas fat percentage between the QCT and CSE-MRI measurements. Bland–Altman analysis was also performed to test the systematic difference between the two measurements. A *p*-value <0.05 was regarded as indicating a statistically significant association. All *p*-values were calculated using a two-tailed significance level. Statistical analysis was performed with the SPSS 13.0 statistical package (SPSS, Chicago, IL, USA).

Results

No participant was excluded from the analysis. The clinical characteristics of the population are summarised in Table 2. The average fat percentages in the CSE-MRI and QCT studies were 2.7±2.6% and -3.6±3.7%, respectively, with a statistically significant difference (*p*<0.0001). For intra-observer precision, the ICC of the MRI measurement was 0.996 (95% confidence interval [CI], 0.994–0.998) for head, 0.995 (95% CI, 0.990–0.997) for body and 0.994 (95% CI, 0.989–0.996) for tail. Meanwhile, the ICC of QCT measurement for intra observer precision was 0.992 (95% CI, 0.986–0.995) for head, 0.993 (95% CI, 0.988–0.996) for body, 0.996 (95% CI, 0.993–0.998) for tail. For interobserver precision, the ICC of the average fat percentages was 0.992

(95% CI, 0.986–0.995) for MRI measurement and 0.994 (95% CI, 0.989–0.996) for QCT measurement. Correlation analysis between the QCT and MRI measurements showed a Pearson correlation coefficient of *r*=0.805 (*p*<0.0001; Fig 3a). Bland–Altman analysis showed that the QCT measurements were systematically lower by 6.3% compared with the CSE-MRI measurements (Fig 3b).

Discussion

CSE-MRI Dixon with measurement of the PDFF can improve the reliability of fat quantification by correcting for confounders such as T2* decay, T1 bias, and noise bias and for the multispectral complexity of fat.¹⁴ The high accuracy of the PDFF-based technique for tissue fat quantification has been used to assess tissue fat content non-invasively in recent years.^{8,15,16} The purpose of this study was to measure the fat content in the pancreas using QCT and to correlate these results with CSE-MRI measurements of pancreatic PDFF. The non-invasive identification of this condition using medical imaging would represent an important step for the treatment-decision process because of the association of increased deposition of fat in the pancreas with the pathogenesis of diabetes and metabolic syndrome.

In the present study of men and women from the general population, the mean pancreatic fat content averaged over all 52 participants measured by CSE-MRI was 2.7±2.6% compared with -3.6±3.7% by QCT. Kuhn *et al.*¹⁷ found a pancreatic fat content of 4.4% in the general population, whereas Singh *et al.*¹⁸ reported higher values and suggested that the threshold between normal and raised pancreatic fat content was 6.2%.

It is interesting to observe that, as expected, the QCT and CSE-MRI measurements showed a good correlation demonstrating that the same parameter (percentage of fat in the pancreas) was quantified by both techniques; however, further studies are required to investigate the systematic differences between the two measurements. Some differences between the two techniques are expected because, while CSE-MRI measures the fat-free pancreatic tissue purely in terms of its water content, QCT additionally measures the non-aqueous components of lean tissue including proteins and minerals; however, other factors are also apparent, including an offset of the zero-point for the QCT percent fat measurement scale compared with the CSE-MRI scale. Further studies would enable these factors to be investigated and adjustments made to the QCT measurements to ensure their consistency with CSE-MRI PDFF.

The present study has some limitations. Firstly, the number of participants was small (*n*=52). Secondly, histopathological confirmation of the accuracy of the pancreatic percent fat measurements obtained by QCT or CSE-MRI imaging was not obtained; however, the primary purpose of the study was to assess the correlation between the QCT and MRI measurements, and biopsy of the pancreas in this healthy population would be unethical. Further studies are required in healthy subjects to establish a normal reference range for QCT measurements of pancreatic fat.

Table 2

The clinical characteristics of the population and fat percentage of the pancreas measured using quantitative computed tomography (QCT) and magnetic resonance imaging (MRI).

Parameters	Total	Male	Female
Age (years)	35.1±7.4	36±5.7	34.3±8.7
Height (cm)	166.3±7.8	172.2±6.6	160.9±4
Weight (kg)	68.4±14.1	77.4±13	60±9
BMI (kg/m ²)	24.8±4.1	26.5±4	23.2±3.5
QCT fat (%)	-3.6±3.7	-2.7±3.8	-4.4±3.5
MRI fat (%)	2.7±2.6	3.4±3.3	2.1±1.6

The data are normally distributed in terms of the mean and standard deviation ($\bar{x} \pm sd$). QCT percentage of fat is the pancreatic fat as measured using QCT. MRI percentage of fat is CSE-MRI proton density fat fraction (%). BMI, body mass index.

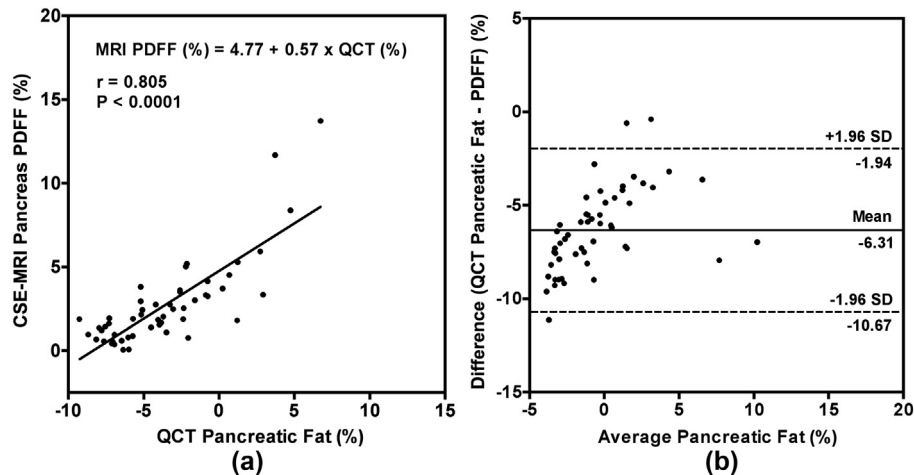


Figure 3 (a) Scatter plot showing the correlation between CSE-MRI measurements of PDFF in the pancreas and QCT measurements of pancreatic fat content with the results of linear regression and Pearson correlation analysis. (b) Bland–Altman plot of the data shown in (a) showing the mean bias and the 95% limits of agreement.

In conclusion, the results of the present study suggest a statistically significant correlation between QCT and CSE-MRI measurements of pancreatic fat content, with QCT measurements systematically lower than the PDFF measurements by 6%.

Conflict of Interests

The authors declare the following financial interests/personal relationships which may be considered as potential competing interests: J Keenan Brown is the employee and stockholders of Mindways Software, Inc.

Acknowledgements

W.J. Yao acknowledges financial support from the Natural Science Foundation of Anhui Medical University (grant number: 2019xkj031).

References

- Covarrubias Y, Fowler KJ, Mamidipalli A, et al. Pilot study on longitudinal change in pancreatic proton density fat fraction during a weight-loss surgery program in adults with obesity. *J Magn Reson Imag* 2019 Jan 30. <https://doi.org/10.1002/jmri.26671>.
- Alswat K, Aljumah AA, Sanai FM, et al. Nonalcoholic fatty liver disease burden - Saudi Arabia and United Arab Emirates, 2017-2030. *Saudi J Gastroenterol* 2018 Jul-Aug;24(4):211–9. https://doi.org/10.4103/sjg.SJG_122_18. Erratum in: *Saudi J Gastroenterol*. 2018 Jul-Aug;24(4):255. PubMed PMID: 29956688; PubMed Central PMCID: PMC6080149.
- Alempijevic T, Dragasevic S, Zec S, et al. Non-alcoholic fatty pancreas disease. *Postgrad Med J* 2017 Apr;93(1098):226–30. <https://doi.org/10.1136/postgradmedj-2016-134546>. Epub 2017 Jan 9. Review. PubMed PMID: 28069746.
- VanWagner LB, Ning H, Allen NB, et al. Twenty-five-year trajectories of insulin resistance and pancreatic β -cell response and diabetes risk in nonalcoholic fatty liver disease. *Liver Int* 2018 Nov;38(11):2069–81. <https://doi.org/10.1111/liv.13747>. Epub 2018 Apr 24. PubMed PMID: 29608255.
- Guglielmi V, Sbraccia P. Type 2 diabetes: does pancreatic fat really matter? *Diabetes Metab Res Rev* 2018 Feb;34(2). <https://doi.org/10.1002/dmrr.2955>. Epub 2017 Oct 26. Review. PubMed PMID: 28984071.
- Gao B, Tsukamoto H. Inflammation in alcoholic and nonalcoholic fatty liver disease: friend or foe? *Gastroenterology* 2016 Jun;150(8):1704–9. <https://doi.org/10.1053/j.gastro.2016.01.025>. Epub 2016 Jan 27. Review. PubMed PMID: 26826669; PubMed Central PMCID: PMC4887345.
- Yang DM, Kim HC, Ryu JK, et al. Sonographic appearance of focal fatty infiltration of the pancreas. *J Clin Ultrasound* 2010;38(1):45–7. <https://doi.org/10.1002/jcu.20632>. Epub 2009/10/01. PubMed PMID: 19790258.
- Tang A, Desai A, Hamilton G, et al. Accuracy of MR imaging-estimated proton density fat fraction for classification of dichotomized histologic steatosis grades in nonalcoholic fatty liver disease. *Radiology* 2015;274(2):416–25. <https://doi.org/10.1148/radiol.14140754>. Epub 2014/09/24. PubMed PMID: 25247408; PubMed Central PMCID: PMC4314291.
- Adams JE. Quantitative computed tomography. *Eur J Radiol* 2009 Sep;71(3):415–24. <https://doi.org/10.1016/j.ejrad.2009.04.074>. Epub 2009 Aug 13. Review PubMed PMID: 1682815.
- Peng Y, Li W, Wang Y, et al. The cut-off point and boundary values of waist-to-height ratio as an indicator for cardiovascular risk factors in Chinese adults from the PURE study. *PLoS One* 2015 Dec 7;10(12):e0144539.
- Cheng X, Blake GM, Brown JK, et al. The measurement of liver fat from single-energy quantitative computed tomography scans. *Quant Imaging Med Surg* 2017 Jun;7(3):281–91. <https://doi.org/10.21037/qims.2017.05.06>. PubMed PMID: 28811994.
- Noller CR. *Chemistry of organic compounds*. 2nd edn. Philadelphia: W B Saunders; 1957.
- ICRU Report 46. *Photon, electron, proton and neutron interaction data for body tissues*. Appendix A. Bethesda: International Commission on Radiation Units and Measurements; 1992. p. 11–3.
- Reeder SB, Hu HH, Sirlin CB. Proton density fat-fraction: a standardized MR-based biomarker of tissue fat concentration. *J Magn Reson Imag* 2012;36(5):1011–4. <https://doi.org/10.1002/jmri.23741>. Epub 2012/07/11. PubMed PMID: 22777847; PubMed Central PMCID: PMC4779595.
- Heber SD, Hetterich H, Lorbeer R, et al. Pancreatic fat content by magnetic resonance imaging in subjects with prediabetes, diabetes, and controls from a general population without cardiovascular disease. *PLoS One* 2017;12(5):e0177154. <https://doi.org/10.1371/journal.pone.0177154>. Epub 2017/05/19. PubMed PMID: 28520813; PubMed Central PMCID: PMC5435170.

16. Meisamy S, Hines CD, Hamilton G, et al. Quantification of hepatic steatosis with T1-independent, T2-corrected MR imaging with spectral modeling of fat: blinded comparison with MR spectroscopy. *Radiology* 2011;**258**(3):767–75. <https://doi.org/10.1148/radiol.10100708>. Epub 2011/01/21, PubMed PMID: 21248233; PubMed Central PMCID: PMC3042638.
17. Kuhn JP, Berthold F, Mayerle J, et al. Pancreatic steatosis demonstrated at MR imaging in the general population: clinical relevance. *Radiology* 2015;**276**(1):129–36. <https://doi.org/10.1148/radiol.15140446>. Epub 2015/02/07, PubMed PMID: 25658037; PubMed Central PMCID: PMC4554208.
18. Singh RG, Yoon HD, Wu LM, et al. Ectopic fat accumulation in the pancreas and its clinical relevance: a systematic review, meta-analysis, and meta-regression. *Metabolism* 2017;**69**:1–13. <https://doi.org/10.1016/j.metabol.2016.12.012>. Epub 2017/03/14, PubMed PMID: 28285638.